NO MONODROMY IN THE CHAMPAGNE BOTTLE (AND SINGULARITIES OF A SUPERINTEGRABLE SYSTEM)

LARRY BATES AND FRANCESCO FASSÒ

Dedicated to Jędrzej Śniatycki on the occasion of his retirement.

Abstract. The three-dimensional champagne bottle system contains no mondromy, despite being entirely composed of invariant two-dimensional champagne bottle systems, each of which posesses nontrivial monodromy. We explain where the monodromy went in the three-dimensional system, or perhaps, where it did come from in the two-dimensional system, by regarding the three-dimensional system not as completely integrable, but as superintegrable (or non-commutatively integrable), and explaining the role of the singularities of its isotropic-coisotropic pair of foliations.

1. Introduction

The 'champagne bottle' system was introduced in [1] to provide a simple example of a completely integrable Hamiltonian system that exhibits monodromy. The system describes a particle in the plane $\mathbf{R}^2 \ni (x, y)$, subject to the central potential

$$V(r) = r^4 - r^2 , \qquad r = \sqrt{x^2 + y^2} .$$

Since the system is rotationally invariant, the angular momentum is conserved and the system is completely integrable. An open dense set in the phase space is fibred by two-dimensional Lagrangian tori, and what is notable is that this fibration is topologically nontrivial. This nontriviality is expressed by saying that the bundle of tori has monodromy, which is an obstruction to the bundle being given the structure of a toral principal bundle [3].

The 'spatial' or '3D' champagne bottle is the analogous problem in three dimensional configuration space, still with $V(r) = r^4 - r^2$, only now $r = \sqrt{x^2 + y^2 + z^2}$. A consequence of the conservation of angular momentum is that the spatial champagne bottle is the (non-disjoint) union of subsystems that are standard, 'planar' or '2D', champagne bottles, and an open dense set of its six-dimensional phase space is still foliated by two-dimensional tori, that are now isotropic. The remarkable fact is that now the tori may be given the structure of a principal bundle. The same is still true if, adopting a common view from complete integrability, one suitably groups together the two-dimensional tori to form bundles of three-dimensional Lagrangian tori. The topological explanation of this, in either case, is simply that

Date: February 24, 2015.

the base of the toral bundle is simply connected, and hence there can be no monodromy.

The aim of this paper is to explain 'where' does the monodromy of the planar champagne bottle go in (or perhaps, come from) the spatial champagne bottle. To this end, we adopt the description of the spatial champagne bottle as a *superintegrable* system, according to which the two-dimensional isotropic invariant two-tori can be naturally arranged to form four-dimensional coisotropic submanifolds.[1] In a dense open subset of the phase space, where the angular momentum is non-zero, these coisotropic submanifolds are diffeomorphic to $P^3 \times S^1$ and are principal two-torus bundles with nonvanishing Chern class. Therefore there is some of topological nontriviality in the two-torus bundle even in the spatial case, but this alone does not explain the appearance of mondromy in the planar subsystems, that is instead related to the presence of exceptional fibres, at zero angular momentum, of the isotropic and coisotropic foliations.

In section 2 we review the properties of the planar champagne bottle and provide a (partially new) proof of the presence of monodromy, which is more geometric than the current ones and sheds some light on the spatial case (and is of independent interest). In section 3, after recalling the general structure of superintegrable systems, we describe it in the case of the spatial champagne bottle and explain which properties of this monodromy-free structure generate the monodromy of its planar subsystems.

2. Précis of known results for the planar champagne bottle.

2.1. **The energy-momentum map.** The two-dimensional champagne bottle [1] system is given by the Hamiltonian

$$h = \frac{1}{2}(p_x^2 + p_y^2) + (x^2 + y^2)^2 - (x^2 + y^2)$$

on the phase space $P = T^*\mathbf{R}^2$, the cotangent bundle of the configuration space $Q = \mathbf{R}^2$. Due to rotational invariance, the angular momentum $j = yp_x - xp_y$ Poisson commutes with h and the system is completely integrable.

The dynamics of the system is easy to describe. There are two types of equilibria and, as in any central force field, motions with zero angular momentum project to radial motions in configuration space and motions with nonzero angular momentum project to rosetta-shaped motions in configuration space. Specifically:

(Eq1) There is a saddle-saddle equilibrium at the origin in P, that together with its stable and unstable manifolds constitutes the crtical set $h = 0$ of the Hamiltonian.

(Eq2) There is a circle of equilibria in P that project over the circle $x^2 + y^2 = 1/2$ in Q, and they form the level set of minimum value $h_{min} = -1/4$ of the Hamiltonian.

(Rad) Non-constant motions with zero angular momentum are periodic, and their radial projection in configuration oscillates on one side of the origin if

[1] For a review of superintegrable systems, see [4].

$h < 0$ (Rad1), symmetrically through the origin if $h > 0$ (Rad2).

Motions with angular momentum $j \neq 0$ are studied via reduction over rotations in the plane. The reduced Hamiltonian is $h_j(r, p_r) = \frac{1}{2}p_r^2 + W_j(r)$, with amended potential $W_j(r) = \frac{j^2}{2r^2} + r^4 - r^2$, and governs the radial motion. It has periodic dynamics, with a single equilibrium point. Reconstruction is trivial in polar coordinates (r, θ) (using $\dot{\theta} = r^{-2} j$) and gives the following:

(Ros) Motions that project over periodic motions of the reduced system project over rosetta-shaped motions in configuration space: the projection in Q is contained in an annulus centered in the origin, winds clockwise if $j < 0$ and counterclockwise if $j > 0$, and its consecutive points of tangency with the outer boundary of the annulus form an angle whose amplitude $\Theta_{j,h}$ varies between 0 and π. Specifically, $\Theta_{j,h}$ tends to 0 when $j \to 0$ with negative h and tends to π when $j \to 0$ with positive h (see figure 1).

(RelEq) The 'relative equilibria' (that project over the equilibrium of a reduced system) are periodic orbits that project to circles in configuration space (and minimize h for given $|j| \neq 0$).

This description is complemented by the geometry of the level sets of the energy-momentum map $J = (j, h) : P \to \mathbf{R}^2$, whose image $R := J(P)$ is the convex region

$$R = \left\{(j, h) |\, j = \pm\sqrt{4r^6 - 2r^4}, h \geq 3r^4 - 2r^2, r \geq 2^{-1/2}\right\}$$

(whose boundary curve is C^3), see figure 1.

Proposition 2.1. *The set of regular values of the energy-momentum map J is the interior of R, except* $(0, 0)$. *For any $(j, h) \in R$, the fibre $J^{-1}(j, h)$ is diffeomorphic to:*

i. *A two-torus, if (j, h) is a regular value. Motions on these tori are as in (Ros) if $j \neq 0$, as in (Rad) if $j = 0$.*
ii. *A circle, if $(j, h) \in \partial R$. Motions are as in (RelEq) if $j \neq 0$, as in (Eq2) if $j = 0$.*
iii. *A pinched circle bundle, if $(j, h) = (0, 0)$ (that is, a singular space homeomorphic to the half-smashed product $S^1 \times S^1/S^1$, which is the product space $S^1 \times S^1$ with a single S^1 collapsed to a point).*[2] *Motions are as in (Eq1).*

We restrict now the consideration to the regular fibres

$$T_{j,h} := J^{-1}(j, h), \qquad (h, j) \in R,$$

of the energy-momentum map (the singular fibres will only be of interest for the comparison with the spatial case). The collection of these two-tori forms a torus bundle over a manifold diffeomorphic to a punctured plane, and, as remarked in [1], this bundle is *not* trivial. For dimensional reasons, this further implies that the bundle is not even a principal bundle, and hence there is an obstruction to the global existence of action variables. This obstruction is called monodromy [3] and may

[2] It is often called a pinched torus, with the pinch being the equilibrium point at the origin.

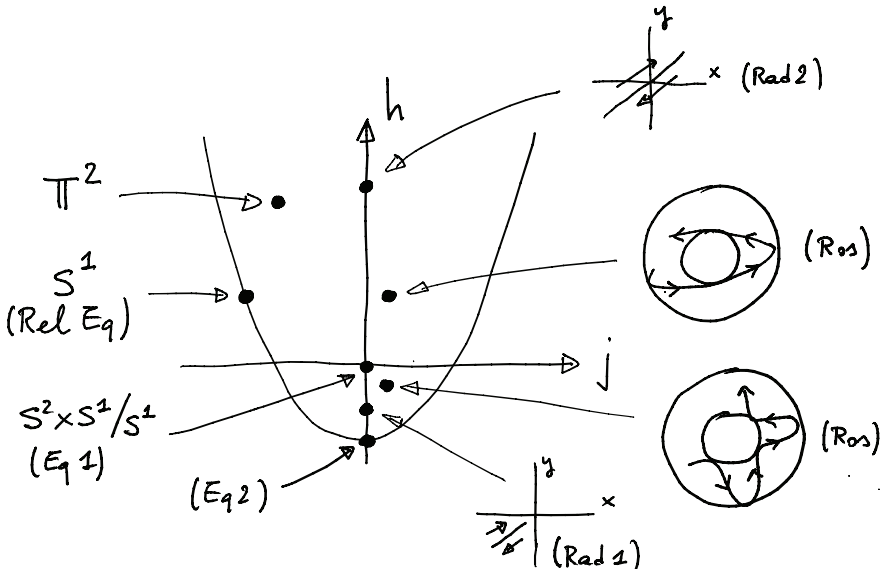

FIGURE 1. The fibres of the energy-momentum map in the planar system and the projections in configuration space of motions with $j \geq 0$ (the projections of motions with $j < 0$ are specular to those with $j > 0$, but oriented clockwise).

be characterized by the fact that the gluing map of the torus bundle is represented, in a suitable basis, by a matrix that is not the identity (up to conjugacy in $\mathrm{GL}(\mathbf{Z}, 2)$).

2.2. **Computing the monodromy.** We compute now the 'monodromy matrix' using an argument that is more topological than those used previously [1, 8] and that introduces a point of view that will be used in the study of the spatial system. Specifically, we compute the change of a homology basis of the two-tori as the base points move along a closed curve that encircles the singular point $(0, 0)$ in the energy-momentum plane.

In so doing, we represent the tori – which belong to the four-dimensional phase space – through their projections to the two-dimensional configuration space Q. There are three cases, depending on the values of j and h, see figure 2.

1. If $j \neq 0$, then the projection of the torus $T_{j,h}$ in Q is an annulus centered on the origin, whose outer and inner radii depend on h and $|j|$. The projection from the torus to the annulus is two-to-one over the interior of the annulus, with the two preimages distinguished by the sign of the radial momentum p_r, and one-to-one on both the inner and outer boundary circles of the annulus. We call the two circles of $T_{j,h}$ that project to the outer and inner boundaries of the annulus the *apocircle* and *pericircle*, respectively. Clearly, these two circles are homotopic (the homotopy can be constructed with the flow of the Hamiltonian vector field of p_r). Motions on these tori project to rosetta-shaped motions.

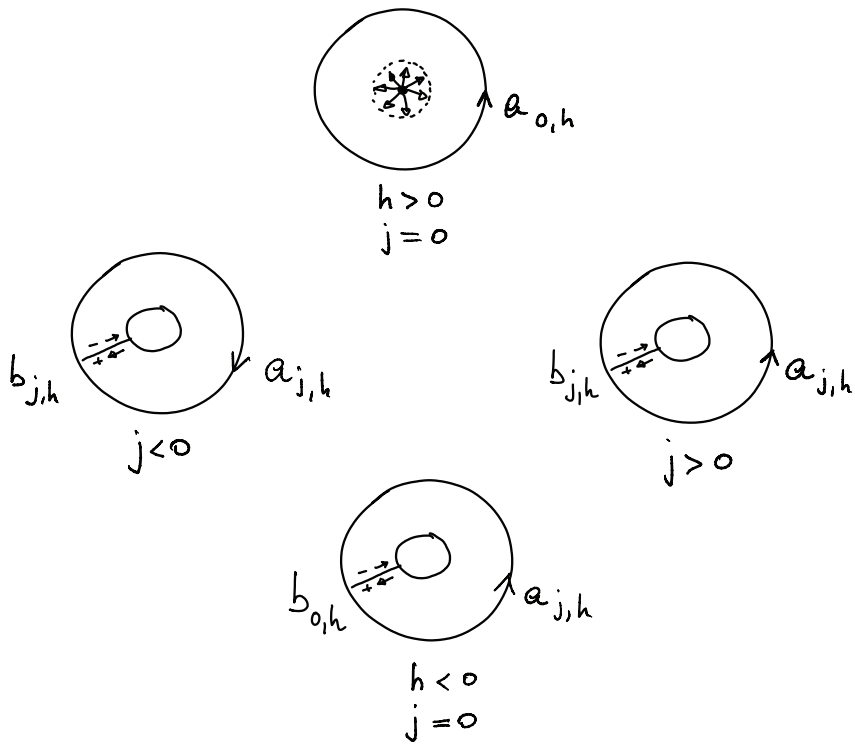

FIGURE 2. Representation in configuration space of the tori $T_{j,h}$ and of the cycles $a_{j,h}$ and $b_{j,h}$ on them.

We choose a basis for the first homology of the tori $T_{j,h}$ with $j \neq 0$, formed by two cycles $a_{j,h}$ and $b_{j,h}$ as follows. Orient the outer boundary of the annulus according to the sign of j, clockwise if $j < 0$ and counterclockwise if $j > 0$,[3] and define $a_{j,h}$ as the apocircle of $T_{j,h}$ oriented according to this orientation of its projection; we call $a_{j,h}$ the *apocycle* of $T_{j,h}$. Next, we choose $b_{j,h}$ as the circle in $T_{j,h}$ that projects to a radial segment of the annulus, oriented according to the sign of p_r; its projection is a radial segment that connects the inner and outer circles. This is illustrated in figure 2, left for $j < 0$ and right for $j > 0$, where a minus sign next to the curve $b_{j,h}$ represents the projection of those points where $p_r < 0$, and a plus sign that of those points where $p_r > 0$.

2. The projection into configuration space of the tori $T_{0,h}$ depends on the value of h. For $h < 0$ the torus still projects over an annulus, two-to-one over the interior

[3]We might as well choose a global orientation in $Q = \mathbf{R}^2$, e.g. the counterclockwise one, but the one we use, even though not defined at $j = 0$, is more suited to the comparison with the spatial system.

and one-to-one over the boundary, see figure 2, bottom. Motions on these tori are periodic motions that project to radial segments which join the outer and inner boundaries of the annulus. Even though we need not use a homology basis for these tori, clearly one is represented by cycles $a_{0,h}$ and $b_{0,h}$ defined as in 1, with the former oriented, e.g., counterclockwise;[4] the cycle $a_{0,h}$ is the *apocycle* of $T_{0,h}$.

3. For $h > 0$, the torus $T_{0,h}$ projects to a disk centered on the origin in Q. The projection is still one-to-one on the boundary of the disk; it is two-to-one in the interior of the annulus with the origin removed, the preimages still distinguished by the sign of p_r; the preimage of the origin is instead an entire circle in $T_{0,h}$, and consists of the momenta of length $|p| = \sqrt{2h}$ that point in all possible directions (in figure 2, top, we represent this circle as a dotted circle of 'vectors', that represent these momenta). Motions on these tori are periodic motions that project to diameters of the disk. Here too, we call *apocycle* of $T_{0,h}$ the circle that projects to the boundary, oriented in a counterclockwise direction. Note that the apocycle is homotopic to the circle in $T_{0,h}$ that projects to the origin, oriented so that the momenta rotate counterclockwise (the homotopy is provided by the flow of the system, for times $0 \le t \le \tau(h)/4$, where $\tau(h)$ is the period of the motions in $T_{0,h}$).

For $j \neq 0$, the cycles $a_{j,h}$ and $b_{j,h}$ depend continuously on the base point (j, h) and, since the tori form a bundle, the limit along a path on the basis of each of them is a cycle on the limit torus. Thus, for each $h \neq 0$, define

$$a_h^{\pm} = \lim_{j\to 0^{\pm}} a_{j,h}\,, \qquad b_h^{\pm} = \lim_{j\to 0^{\pm}} b_{j,h}$$

which are cycles on $T_{0,h}$. From figure 2 it is clear that

$$\begin{aligned} a_h^+ &\sim -a_h^-\,, \qquad h \neq 0 \\ b_h^+ &\sim b_h^-\,, \qquad h < 0 \end{aligned} \tag{1}$$

(specifically, $a_h^+ \sim a_{0,h}$ and $b_h^+ \sim b_{0,h}$). However, contrary to what one might perhaps at first think, for positive h it is not $b_h^+ \sim b_h^-$ but

$$b_h^+ \sim b_h^- + a_h^-\,, \qquad h > 0\,. \tag{2}$$

The simplest way to prove (2) is to let the dynamics do the work, see figure 3 (where for greater clarity the annuli are shown also for $h < 0$). For $j \neq 0$ the cycle $b_{j,h}$ is homologous to the curve formed by the following two oriented curves. One is the arc $\omega_{j,h}$ of a dynamical orbit in $T_{j,h}$ whose endpoints P, P' are two consecutive contact points with the apocycle $a_{j,h}$, oriented according to time. The second is the arc $\alpha_{j,h}$ of $-a_{j,h}$ that joins P and P' (oriented opposite to $a_{j,h}$). By the continuity of the flow, as $j \to 0$ the oriented curve $\omega_{j,h}$ in $T_{j,h}$ tends to a curve y_h in $T_{0,h}$ which is half of the dynamical orbit on $T_{0,h}$, oriented according to time, with initial point on that point of the apocycle of $T_{0,h}$ whose projection is aligned with the projection of P. The same happens for $j < 0$, but now the orientation of the cycle $a_{j,h}$ is reversed. Since, as noticed, when $h > 0$ the angle $\Theta_{j,h}$ between the projections of P and P' tends to π as $j \to 0$, it follows that the limits $b_h^{\pm}$ of the cycles $b_{j,h}$ are homotopic

[4]The choice of the orientation of the apocycle at $j = 0$ is immaterial.

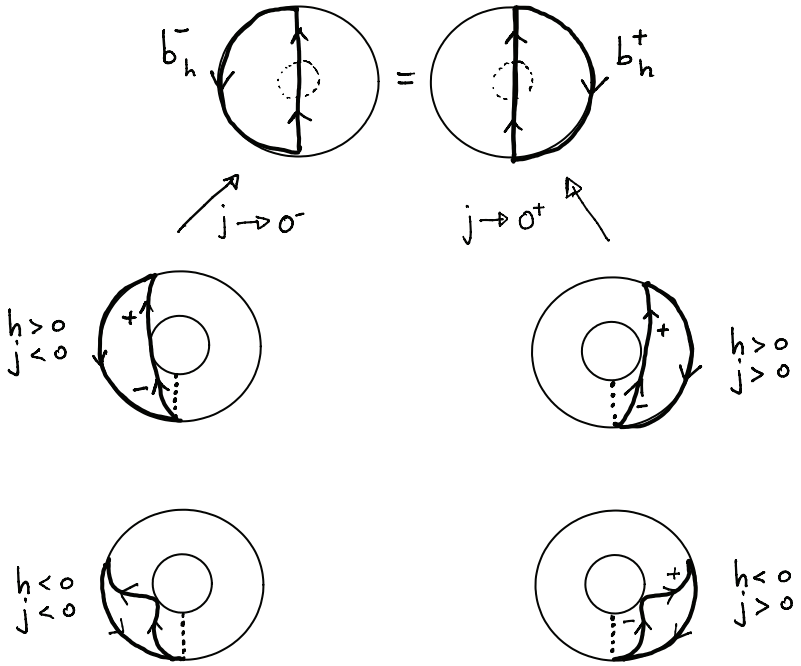

FIGURE 3. Circles homotopic (thick) to $b_{j,h}$ (dotted) for positive and negative j and h and their limits (thick) for $j \to 0^\pm$, $h > 0$.

to the closed curves in $T_{0,h}$ formed by y_h followed by half of $-a_h^\pm$. Thus b_h^+ and b_h^- differ by a_h^-, see figure 3.

Formulas (1) and (2) give

$$\begin{pmatrix} a_h^- \\ b_h^- \end{pmatrix} = \begin{pmatrix} -1 & 0 \\ 0 & 1 \end{pmatrix} \begin{pmatrix} a_h^+ \\ b_h^+ \end{pmatrix} \quad \text{if } h < 0\,, \qquad \begin{pmatrix} a_h^+ \\ b_h^+ \end{pmatrix} = \begin{pmatrix} -1 & 0 \\ 1 & 1 \end{pmatrix} \begin{pmatrix} a_h^- \\ b_h^- \end{pmatrix} \quad \text{if } h > 0$$

and the monodromy matrix of this bundle is

$$\begin{pmatrix} -1 & 0 \\ 0 & 1 \end{pmatrix} \begin{pmatrix} -1 & 0 \\ 1 & 1 \end{pmatrix} = \begin{pmatrix} 1 & 0 \\ 1 & 1 \end{pmatrix}$$

in this basis.

We conclude the analysis of the planar case with two observations. The first is that the previous analysis seems to point to a special role of the fibres with $j = 0$ and $h > 0$ in the appearance of monodromy. Further insight on this will come from the analysis of the spatial system. The second observation is that a reasoning similar to the one just done shows that, for any $h \neq 0$,

$$\begin{aligned} &\lim_{j \to 0^\pm} b_{j,h} = x_h && \text{if } h < 0 \\ &\lim_{j \to 0^\pm} (a_{j,h} + 2b_{j,h}) = x_h && \text{if } h > 0 \end{aligned} \tag{3}$$

where x_h is the cycle formed by a periodic orbit on $T_{0,h}$, oriented according to time.

Remarks: 1. It is known that if a two-torus bundle has a singular fibre which is a pinched torus, then the bundle in a neighbourhoud of the singularity has monodromy.

2. The cycle b is typically used for the definition of the second action, as it corresponds to $\oint p_r\, dr$. It is then clear why this action is not globally defined.

3. The spatial champagne bottle as a superintegrable system

In the three-dimensional case, the configuration space is $Q = \mathbf{R}^3$ and

$$h = \frac{1}{2}(p_x^2 + p_y^2 + p_z^2) + (x^2 + y^2 + z^2)^4 - (x^2 + y^2 + z^2)^2$$

is the Hamiltonian on the phase space $P = T^*Q = T^*\mathbf{R}^3$. The conserved angular momentum is $j = q \times p$, so now there are four conserved quantities j_x, j_y, j_z, h. As in any generic central force problem with bounded motion, motions with non-zero angular momentum are generically quasi-periodic on isotropic tori of dimension two. Motions with zero angular momentum are either equilibria or collinear with the origin, and in the latter case they are periodic if $h \neq 0$.

A common approach to studying such a system is to treat it as Liouville integrable by choosing three commuting first integrals such as h, j_z and $|j|$. This provides an open dense connected set of three-dimensional Lagrangian tori on which the motion takes place. However, we will not follow this approach here. There are at least two good reasons for this.[5] First, the selection of the three-torus is somewhat arbitrary, as the motion lies on a two-torus, and consequently there is no intrinsic dynamical meaning to the choice of three-torus. Secondly, any such choice involves surgery by discarding some subset of the phase space. A preferred approach looks at the whole of phase space and incorporates the obvious rotational symmetry of the problem. In this way we are forced to consider the three-dimensional champagne bottle as a *superintegrable* system, which we take up in the next section.

3.1. Structure of superintegrable systems.

The essential feature of a superintegrable system is that it contains more integrals than necessary for complete integrability, and these integrals define a Poisson structure with certain properties.[6] This has two important consequences. The first, and most obvious, is that the motion lies on sets of dimension lower than the number of degrees of freedom, which are often tori. The second, and often overlooked, is that these lower dimensional invariant setes are naturally arranged with respect to the stratification of the Poisson structure defined by the first integrals. As our main interest here is to illuminate the champagne bottle from this point of view, we only list the few results we use, and refer the reader to the many more details of this theory which may be found in

[5] For a discussion of the issues involved here, see [4].

[6] Properties that ensure the existence of the set of symmetries complementary to the first integrals that are needed for integrability.

the original articles of Nekhoroshev [7] and Mischenko and Fomenko [6], and in the review article [4].

In general, the idea is as follows. Consider a Hamiltonian system on a $2n$-dimensional symplectic manifold (P, ω) with $2n-k$ first integrals of motion $f_1, \ldots, f_{2n-k}$. Denote

$$f = (f_1, \ldots, f_{2n-k}) : P \to B = f(P) \subset \mathbf{R}^{2n-k} .$$

Assume that there is an open set $P_{reg} \subset P$ such that $f : P_{reg} \to B_{reg} := f(P_{reg})$ is a submersion with compact connected fibres. Suppose further that there exist functions $\pi_{rs} : B \to \mathbf{R}$ such that the Poisson brackets satisfy

$$\{f_r, f_s\} = \pi_{rs} \circ f, \qquad r, s = 1, \ldots, 2n-k. \tag{4}$$

The Nekhoroshev-Mischenko-Fomenko theorem asserts that if the matrix c with entries π_{rs} has constant rank $2n-2k$ everywhere in B_{reg}, then the fibres in P_{reg} of the map f are k-dimensional isotropic tori. Moreover, each fibre in P_{reg} has a neighbourhood endowed with a system of 'partial' or 'generalized' action-angle coordinates $(I, \theta, p, q) \in \mathbf{R}^k \times \mathbf{T}^k \times \mathbf{R}^{n-k} \times \mathbf{R}^{n-k}$ such that the symplectic form has the local expression $dI_j \wedge d\theta^j + dp_m \wedge dq^m$ and the Hamiltonian of the system depends only on the actions I.

The first consequence of this theorem is that the dynamics in P_{reg} is conjugate to linear dynamics on the k-dimensional tori, which in these coordinates are given by $(I, p, q) =$ constant. Furthermore, the base B_{reg} of the fibration by k-tori is a Poisson manifold of rank $2n-2k$ with the Poisson bracket (4), and so is foliated by $(2n-2k)$-dimensional symplectic leaves. Consideration of the sets of all tori in the preimage of a symplectic leaf gives a second, coarser, coisotropic foliation of P_{reg}. Under certain regularity conditions, the symplectic foliation is a fibration

$$c : B_{reg} \to C_{reg} := c(B_{reg}) \subseteq \mathbf{R}^k ,$$

where the components $c_1, \ldots, c_k$ of c are the Casimirs of the base B_{reg}, and the restrictions of this foliation to the individual coisotropic leaves of P_{reg} are k-torus bundles, that may be regarded as the fibres of the composed map

$$\hat{c} := c \circ f : P_{reg} \to C_{reg} .$$

The global geometry of the regular part of this pair of foliations of P_{reg} is discussed by Dazord and Delzant [2]. In particular, there is a generalized notion of monodromy, which is the obstruction to the fibration of P_{reg} by k-tori being a principal bundle. Monodromy always vanishes if the Casimir space C_{reg} is simply connected. Even in the absence of monodromy, the fibration by tori may be nontrivial. In particular, the fibration of the individual coisotropic leaves may have nonzero Chern class.

In specific examples, there are typically singularities of the foliation by tori and of the symplectic foliation in $P \backslash P_{reg}$ and $B \backslash B_{reg}$, respectively. A general study of these singularities is still missing.

This structure is symbolically represented in figure 4, and explains why the leaves of the coisotropic foliation are called *flowers*, and the tori in a flower are the *petals*.

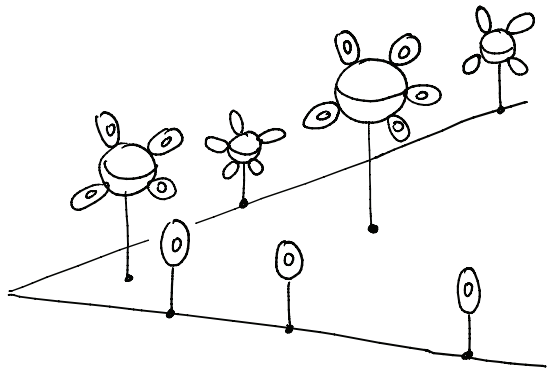

FIGURE 4. Representation of the two foliations of a superintegrable system, with singularities (of the flowers and of the petals).

We now elucidate these two foliations, and their singularities, for the spatial champagne bottle.

3.2. **The isotropic foliation in the 3D Champagne bottle.** By virtue of being a central force problem, the three-dimensional champagne bottle is composed entirely of invariant two-dimensional champagne bottle systems. This allows us to more or less take the results from the two-dimensional case and write down the analogous results for the three-dimensional case by doing little more than considering the action of the rotation group.

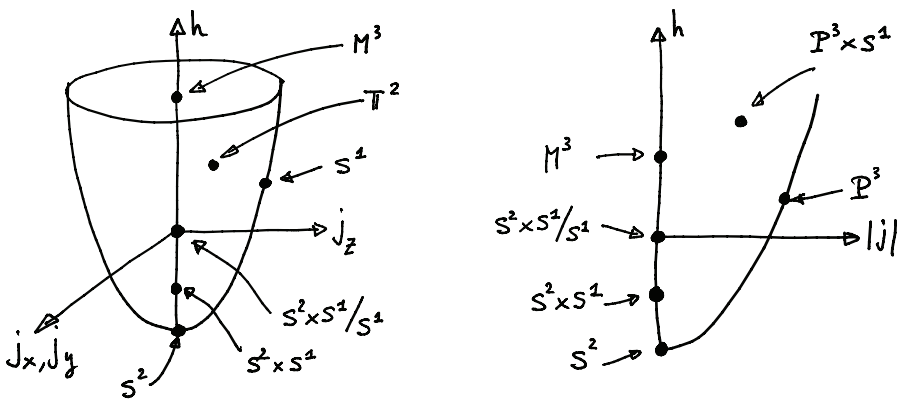

FIGURE 5. The fibres of the energy-momentum map (left) and the Casimir map (right) in the spatial system.

In the spatial system, the isotropic foliation is given by the energy-momentum map $J : P = \mathbf{R}^6 \to \mathbf{R}^4 : (q, p) \to (j, h)$, whose image is the region B defined by

$$B := \left\{(j, h) \mid |j| = \pm\sqrt{4r^6 - 2r^4}\,,\ h \geq 3r^4 - 2r^2\,,\ r \geq 2^{-1/2}\right\}$$

and sketched in figure 5, left. The fibres of the energy-momentum map J, and their dynamical meaning, are described by the following proposition (the motions on each fibre are easily inferred from the planar case):

Proposition 3.1. *The fibre of the energy-momentum map J over a value $(j, h) \in B$ is diffeomorphic to:*

i. *An isotropic torus T^2 at each regular value of the energy-momentum map (interior of B, with the h-axis removed).*
ii. *S^1, if $(j, h) \in \partial B$, and $j \neq 0$.*
iii. *S^2, if $j = 0$ and $h = h_{min}$.*
iv. *$S^2 \times S^1$, if $j = 0$ and $h_{min} < h < 0$.*
v. *M^3, if $j = 0$ and $h > 0$. The manifold M^3 is the nontrivial principal circle bundle over the projective plane P^2 which is associated to the canonical line bundle over the projective plane.*
vi. *A pinched circle bundle, if $(j, h) = (0, 0)$. (This is a singular space homeomorphic to the half-smashed product $S^2 \times S^1/S^2$, which is the product space $S^2 \times S^1$ with a single S^2 collapsed to a point).*

Furthermore, all fibres with $j = 0$ are Lagrangian.

Proof. The only item in the list that may require explanation is the manifold M^3. This is most easily seen dynamically. Consider a motion of the particle with positive energy and zero angular momentum. The motion is periodic, back and forth along a straight line segment in the configuration space Q that is symmetric through the origin. The trajectory as it sits in phase space is identified with the circle S^1, and oriented by the direction of motion. The collection of all such symmetric segments of a given fixed length (determined by the value of the energy) form a manifold diffeomorphic to the projective space P^2. The identification of this circle bundle with the canonical line bundle is seen by recalling the construction of the canonical line bundle using the lines that determine the projective space itself (see [5].)

When $j = 0$, q and $p = \dot{q}$ are parallel; but for a central force, $\dot{p}$ is parallel to q and hence to $\dot{q}$; thus the restriction of $dp_i \wedge dq^i$ to $j = 0$ vanishes. q.e.d.

The set B_{reg} of regular values of the energy-momentum map is the interior of B with the line $j = 0$ removed. Since it is simply-connected, the bundle of two-dimensional tori over B_{reg} is a principle bundle. However, B_{reg} is not contractible, but retracts onto a two-sphere S^2, which may be taken to be a leaf of the symplectic foliation discussed in the next subsection. Compared to the planar case, one reason for this is the higher dimensionality of the base of the bundle. But in addition, in the spatial system the set of singularities of the foliation by the level sets of J includes all motions with zero angular momentum, not just the equilibria ($h = h_{min}$) and the saddle-saddle point with its stable and unstable manifolds ($h = 0$) as in the

planar system. In this way, the fibres that are 'responsible' for the appearance of monodromy in the planar case are no longer part of the regular set in the spatial case. Dynamically, motions with $j = 0$ and $h \neq h_{min}, 0$ are periodic both in the planar system and in the spatial systems. In the planar system, however, for each h, there is a unique, natural way of collecting these periodic orbits together to form a two-torus, that fits smoothly in the fibration by two-tori defined by the dynamics. In the spatial case, instead, there is no unique way of choosing a plane at zero angular momentum. Further insight on these singularities is gained by considering the coisotropic foliation, and the foliation of its leaves by the invariant tori.

3.3. **The coisotropic and symplectic foliations in the 3D Champagne bottle.** In the spatial Champagne bottle system, the Poisson brackets of the angular momentum and of the Hamiltonian give the structure of a Poisson manifold to the interior $B^\circ = B \backslash \partial B$ of $B = J(P)$, and a choice of (global) Casimirs is $|j|$ and h. The manifold B° is larger than B_{reg}, since it includes also the points with $j = 0$, and the rank of the Poisson structure, which is two at all points of B_{reg}, drops to zero in $B^\circ \backslash B_{reg}$, that is, where $j = 0$:

Proposition 3.2. *The symplectic leaves of B° are two-dimensional spheres in B_{reg} and points in $B^\circ \backslash B_{reg}$.*

Note that each regular symplectic leaf, based on a point $(|j|, h)$ with $|j| \neq 0$, may be identified with the sphere of radius $|j|$ centered at the origin in the angular momentum space $j \in \mathbf{R}^3$.

The image $C = c(B) = \hat{c}(P) \subset \mathbf{R}^2$ of the Casimir maps

$$c : B \to \mathbf{R}^2 : (j, h) \mapsto (|j|, h)\,, \qquad \hat{c} = c \circ J : P \to \mathbf{R}^2\,,$$

is the half of the image of the energy-momentum map of the planar champagne bottle defined by $j \geq 0$, see figure 5, right.

Proposition 3.3. *The set of regular values C_{reg} of the Casimir map $\hat{c} : P \to C$ is the interior of C (and coincides with $c(B_{reg})$). The fibre $\hat{c}^{-1}(|j|, h)$ is diffeomorphic to:*

i. *$P^3 \times S^1$, if $(|j|, h) \in C_{reg}$.*
ii. *P^3, if $(|j|, h) \in \partial C$ and $|j| \neq 0$.*
iii. *$J^{-1}(0, h)$, if $|j| = 0$ and $h \geq h_{min}$.*

Proof. (ii) For each $j \in \mathbf{R}^3$ with the given norm, the intersection between $\hat{c}^{-1}(|j|, h)$ and the subset of phase space where the angular momentum is j is a circle orthogonal to j. Varying j in $\mathbf{R}^3$ gives a manifold diffeomorphic to $T_1 S^2$, or P^3.

(i) The argument used to prove item (ii) implies that the set of apocycles of the tori contained in the regular fibre $\hat{c}^{-1}(|j|, h)$ is diffeomporphic to P^3. Acting on this set with the flow of p_r produces a set diffeomorphic to $P^3 \times S^1$ and that coincides with $\hat{c}^{-1}(|j|, h)$.

(iii) If the symplectic leaf is a point then the fibre of the Casimir map coincides with that of the energy-momentum map. q.e.d.

The set C_{reg} of regular values of the Casimir map $\hat{c} : P \to \mathbf{R}^2$ is contractible, so the bundle of regular coisotropic fibres (the flowers) is trivial. However, there is some nontriviality in the structure of the individual flowers themselves.

In fact, the regular flowers, diffeomorphic to $P^3 \times S^1$, are fibred by the isotropic two-tori over a base which is a regular symplectic leaf diffeomorphic to S^2. This fibration is the composition of two fibrations: the trivial fibration $P^3 \times S^1 \to P^3$, and a fibration $P^3 \to S^2$. The former fibration is given by the flow of p_r (see the proof of the last proposition), and its fibres are homotopic to the b-cycles of the tori of the planar case. The latter fibration is given by the rotations around the direction of the angular momentum, and is topologically not trivial; its fibres are homotopic to the a-cycles of the tori of the planar subsystems. At variance from the planar case, the latter fibration does not have a global section (there is no global choice of a point on the 'apocycles') and the resulting fibration is the Hopf fibration, which has a nontrivial Chern class.

At first sight, it might be thought that the monodromy of the planar system is manifesting in the topology of the regular part of the torus bundle of the spatial system. Since the set of regular values of the energy-momentum map is simply-connected, any obstruction to the triviality of the torus bundle would live in the higher homotopy of the base. In this case, it just so happens that the base retracts onto a symplectic leaf, that also serves as the base of a flower. From this point of view, the monodromy would have manifested itself as the Chern class of a toral bundle. However, there are at leat two reasons why this fact, alone, cannot be considered the source of monodromy. The first is that it does not explain how the monodromy of the two-dimensional problem, which is an obstruction to the two-torus bundle being a principal bundle, can manifest itself as a nonzero Chern class of a principal bundle. At a more specific level, the second reason is that the angle associated to the nontrivial S^1-fibration of the flower $P^3 \times S^1$ reduces, in the planar case, to the angle along the orbits of the rotation group in the plane, which is a globally defined angle. In the planar case it is rather the cycle given by the flow of p_r, which is not globally defined, that is related to the presence of monodromy.

This point of view misses the crucial fact that, in the spatial system, the regular parts of the flower and petal bundles do not contain motions with zero angular momentum. It is precisely the operation of continuing, when $h > 0$, the b-cycles through the exceptional fibres at $j = 0$ (an operation that has no meaning in the spatial system) that is at the basis of the appearence of the monodromy in its planar subsystems. W now look into this process from the perspective of the spatial system.

3.4. **Monodromy from toral accumulation in the exceptional fibres.** Choose an orthonormal basis $\{e, e', e''\}$ of $\mathbf{R}^3$, and consider the planar subsystem whose motions take place in the plane $e'e''$, orthogonal to e. For given h, each two-torus of this planar subsystem with nonzero angular momentum is a regular fibre of the energy-momentum map of the spatial system. The planar subsystem intersects each regular fibre $\hat{c}^{-1}(|j|, h)$, $j \neq 0$, of the coisotropic foliation in two distinct two-tori (which are based on the points $(\pm j, h)$ of the symplectic leaf $c^{-1}(|j|, h)$) and

intersects the exceptional fibres at $|j| = 0$ of the coisotropic foliation in a single two-torus (formed, as discussed, by all radial periodic motions of energy h in the $e'e''$ plane). We now examine how the pair of tori in the regular flowers coalesce into a single torus in the exceptional flower as $|j| \to 0$, when $h > 0$.

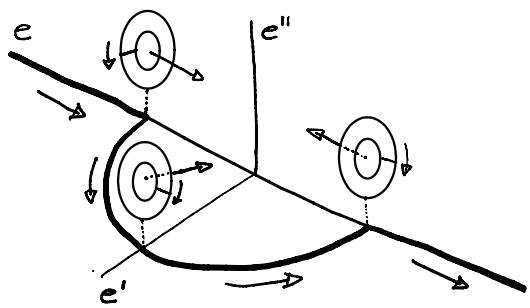

FIGURE 6. The projection of the half-turn

To this end, we restrict ourselves to a subspace of constant, positive h of the energy-momentum space B. In this subspace, consider the line through the origin and parallel to e. A small deformation of this line, that does not contain the exceptional fibre at $j = 0$, is base to a trivial torus bundle. For instance, fix some $\lambda > 0$ and, as in figure 6, replace the segment $|j| < \lambda$ of the line with a half-circle of radius λ which is centered on $j = 0$ and lies in the plane spanned by e and e'. The fibre of the energy-momentum map over each point (j, h) of the half circle is a two-torus that projects, in the configuration space Q, to an annulus orthogonal to j.

The limit $j \to 0$ produces a one-parameter family of two-tori in the exceptional fibre at $j = 0$ (the one diffeomorphic to M^3). These limit tori project in configuration space to a one-parameter family of disks that rotate by an angle π around the e'' axis. The tori at the endpoints of this limit family are the same torus and, in the limit, the a and b cycles of the tori at the endpoints of the half-circle have different limits in this common limit torus. Following the rotation of the disk through the family of tori along the half-circle, as in figure 5, makes clear why these limits of the a and b cycles are as in (1), (2) (for the b-cycle, replace the circle with the two arcs ω and α as explained in section 2.2, and observe that the effect of the rotation of the disk is precisely that of mapping the curve on the top-right disk to that of the top-left disk of figure 3).

Remark: The heart of the present argument is the invariance under rotation of the 3D champagne bottle. In general, if the map f of the first integrals of a superintegrable system is the energy-momentum map of a Hamiltonian action of a Lie group G that leaves the Hamiltonian invariant, then the flowers are G-invariant and the G-action maps petals onto petals of the same flower. Thus, in the 3D

champagne bottle, the rotation group SO(3) allows the identification of all tori based on the same symplectic leaf. In this way, the cycles from the torus at one of the endpoints of the half-circle may be transported to the torus at the other endpoint, and compared. The limit is then taken in the same torus, and again leads to (1), (2). Clearly, an argument of this type might be used to compute the monodromy of the planar champagne bottle, using a reflection instead of the rotations; we leave this analysis for a separate work, because it has an interest and implications that go beyond those of the present work.

References

[1] L. Bates. Monodromy in the champagne bottle. *Journal of applied mathematics and physics (ZAMP)*, 42:837–847, 1991.

[2] P. Dazord and T. Delzant. Le probleme general des variables actions-angles. *Journal of differential geometyry*, 26:223–251, 1987.

[3] J. Duistermaat. On global action-angle coordinates. *Communications on Pure and Applied Mathematics*, 33(6):687–706, 1980.

[4] F. Fassò. Superintegrable Hamiltonian systems: Geometry and perturbations. *Acta Applicandae Mathematicae*, 87(1-3):93–121, 2005.

[5] J. Milnor and J. Stasheff. *Characteristic classes*. Number 76 in Annals of mathematics studies. Princeton university press, 1974.

[6] A. Mischenko and A. Fomenko. Generalized Liouville method of integration of Hamiltonian systems. *Funct. Anal. Appl*, 12:113–121, 1978.

[7] N. Nekhoroshev. Action–angle variables and their generalizations. *Trans. Moskow Math. Soc.*, 26:180–198, 1972.

[8] M. Winnewisser, B.P. Winnewisser, F.C. De Lucia I.R. Medvedev, S.C. Ross, and L.M. Bates. The hidden kernel of molecular quasi-linearity: Quantum monodromy. *Journal of Molecular Structure*, 798:1–26, 2006.

Larry M. Bates
Department of Mathematics
University of Calgary
Calgary, Alberta
Canada T2N 1N4
bates@ucalgary.ca

Francesco Fassò
Università di Padova
Dipartimento di Matematica
Via Trieste, 63
35121 Padova, Italy
fasso@math.unipd.it